



Heat and Fluid Flow Enhancement of the Structure of a Solar Air Heater with Optimized Distance Between Rib and Groove

Abolfazl Hajizadeh Aghdam^{a,*}, Hossein Dolatabadi^b

^{a,b} *Department of mechanical engineering, Arak University of Technology, Arak 38181-41167, Iran*

ARTICLE INFO

Received: 2019.09.22
Received in revised form:
Accepted: 2019.10.02
Available online:

Keywords:

Optimization;
Rib and Groove;
Heat Transfer;
Pressure Drop

ABSTRACT

A popular and common method to enhance the heat transfer in a flow passage is to artificially roughen the surfaces with ribs, grooves or combination of ribs and grooves (rib-grooved surface). In this paper, heat transfer enhancement of optimized rib-grooved surfaces in channels is multi objectively optimized applying the NSGA II algorithm. The distance between rib and groove was set from 0 to 3w. The optimized distance between rib and groove was $d=2.2w$ which computed by considering maximum heat transfer and minimum friction factor, simultaneously. The effects of Reynolds number of 5000 to 30000 are so investigated. when the velocity of flow increases the Nusselt number and pressure drop increase. When the distance between rib and groove increases the Nusselt number increased while the friction factor decreases in optimization with NSGAI algorithm point= $2.2w$ was the best.

1. Introduction

A popular and common method to enhance the heat transfer in a flow passage is to artificially roughen the surfaces with ribs, grooves or combination of ribs and grooves (rib-grooved surface). The artificial roughness is often used in heat exchanger systems, such as solar air heaters, nuclear reactors, electronic cooling devices and gas turbine blades [1-10]. The flow around the ribs and grooves is characterized by recirculation, reattachment and secondary flow. These factors functionally disrupt laminar sub layer and hence improve heat transfer. In fact, the ribs, grooves and their combination increase the fluid flow turbulence near the wall by breaking the laminar sub layer and create local wall turbulence due to flow separation and reattachment, which disrupt the thermal boundary layer

and reduce the thermal resistance and greatly enhance the heat transfer [11-13]. Numerical or experimental studies on ribs and grooves have paid attention to configuration parameters such as rib and groove shape, scale, angle of attack, pitch, channel shape and so forth [14-23]. However, the use of artificial roughness results in higher friction and hence higher pumping power requirements. Therefore, it is desirable that the turbulence should be created in the vicinity of the wall, i.e. only in the laminar sub-layer region, which is responsible for thermal resistance. Hence, the efforts of researchers have been directed towards finding the roughness shape and arrangement, which break the laminar sub layer, enhance the heat transfer coefficient most with minimum pumping power penalty.

The correlations for heat transfer coefficient and friction factor developed for solar air heater ducts having artificial

roughness of different geometries were reviewed by Kumar et al. [24]. Manca et al. [25] presented a numerical investigation on air forced convection in a rectangular channel with constant heat flux applied on the bottom and upper external walls. It was reported that the trapezoidal-shaped ribs with decreasing height in the flow direction give the best heat transfer enhancement performance. A comprehensive study on the effect of different shape of the ribs on heat transfer enhancement and pressure drop has been done by Moon et al [26]. They reported that the new boot-shaped rib gave the best heat transfer performance with an average friction loss performance, and the reverse pentagonal rib gave the best friction loss performance.

Addition of grooves in between adjacent square ribs enhances the heat transfer capability of the surface and Nusselt number can be further enhanced beyond that of ribbed duct while keeping the friction factor enhancement low [2,16,27,28]. Al-Shamani et al. reported that trapezoidal-shaped grooves give the best heat transfer enhancement performance [28].

However, the heat transfer performances of many rib-grooved shapes with different distance have not yet been reported. In the present work, the flow structures, heat transfer characteristics, and thermal performances of new combination of rib-grooved rectangular channels shapes (boot-shaped rib and trapezoidal groove) with different distance over Reynolds number in the range of 5,000–30,000 were evaluated using 2D RANS analysis.

The objectives of this research are to assess the occurrence of hot spots on the roughened wall by investigating the effects of rib-grooved shapes on the local heat transfer and to achieve optimized distance between rib-grooved for the best thermal performance and pumping power.

2. Materials and Methods

The configuration of the rib-grooved shapes (boot-shaped rib and trapezoidal groove) used in this study is shown in Fig.1. The rib and groove height (e) is equal to the rib and groove width (w). The computational domain consists of a 1000 mm long smooth section followed by a rib-grooved roughened section of equal length. The hydraulic diameter D_h of 25.5 mm is considered. To ensure that the fully developed flow is formed at the inlet of roughened region and reversed flow does not appear at the outlet, both upstream and downstream region are extended near 20 times of channel height. The rib height-to-hydraulic diameter ratio, e/D_h , is 0.1 and rib-groove distance, d , varies from 0 to $3w$ which it is common range in the roughened surfaces. A combined structured and unstructured grid system was used to mesh the models for the CFD simulations as shown in Fig.2.

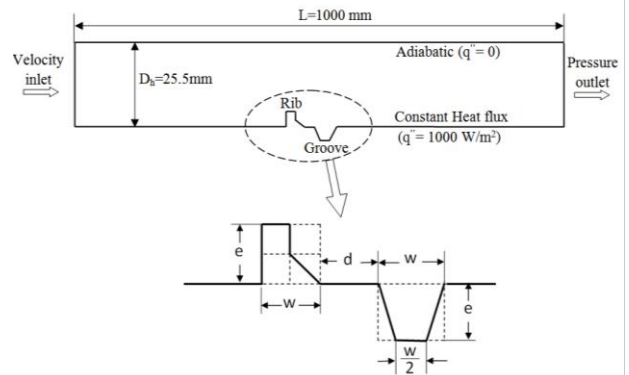


Figure 1: geometry of rib-grooved channel

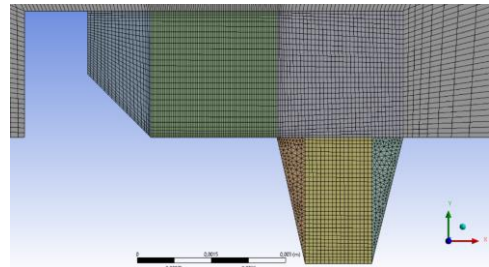


Figure 2: grid system mesh element for solving CFD model

The numerical analysis of thermal behaviors and flow dynamic characteristics for the rib-grooved channel has been carried out to predict the performance of heat transfer and pressure drop. The governing equations are solved using a finite volume approach. The time-independent incompressible Navier–Stokes equations and the turbulence model are discretized using the finite volume method. Many investigators predicted the turbulent forced convection in a rectangular duct with periodic ribs, grooves and rib-grooves by utilizing different turbulence models, such as the $k - \epsilon$, $k - \omega$, Reynolds stress model (RSM) and large eddy simulations (LES) models. The RSM model can offer more accurate results than the two-equation models when predicting flow patterns of revolving flows [26, 29].

In the present study, the $k - \epsilon$ model is used for the turbulence modeling, and the SIMPLE algorithm is used to handle the pressure-velocity coupling. The discretized nonlinear equations are implemented implicitly. To evaluate the pressure field, the pressure-velocity coupling algorithm SIMPLE (Semi Implicit Method for Pressure-Linked Equations) is selected.

The following assumptions are applied through the simulations: the flow is steady, fully developed turbulent and two dimensional, the thermal conductivity of the channel wall and material roughness does not change with temperature, and the channel wall and material roughness

are homogeneous and isotropic with enhanced wall treatment function.

The solutions were considered to be converged when the normalized residual values were less than 10^{-6} for all variables but less than 10^{-4} only for the continuity equation. . Chaube et al. [30] suggested that the calculation with two dimensional flow model yields the results closer to measurements as compared that with three dimensional flow. In this work, the 2D flow is therefore carried out for saving computer memory and computational time.

2. Materials and Methods

The physical properties of air have been assumed to remain constant at average bulk temperature. Impermeable boundary and no-slip wall conditions have been implemented over the channel walls as well as the ribs and grooves. As the boundary condition for the computational domain shown in Fig. 1, a uniform velocity profile was adopted at the inlet with a Reynolds number of 5000 to 30,000 based on the channel hydraulic diameter. The inlet temperature of the working fluid (air) was kept constant at 298.15 K, and a specific pressure was adopted at the outlet. A Uniform heat flux condition (1000 W/m²) is applied to the roughened wall (lower wall), While all the other surfaces are regarded as adiabatic.

Three parameters of interest in the present work are the Reynolds number, friction factor and Nusselt number.

$$Re = \frac{\rho u D_h}{\mu} \quad (1)$$

The friction factor, f is computed by pressure drop, ΔP across the length of the duct, L as

$$f = 2 \frac{\Delta P}{L} \left(\frac{D_h}{\rho u^2} \right) \quad (2)$$

The heat transfer is measured by local Nusselt number which can be written as

$$Nu_x = \frac{h_x D_h}{k} \quad (3)$$

The average Nusselt number can be obtained by

$$Nu = \frac{1}{L} \int Nu_x \partial x \quad (4)$$

Genetic Algorithm is optimization method based on the mechanics of natural genetics and natural selection. Genetic Algorithm mimics the principle of natural genetics and natural selection to constitute search and optimization procedures. GA is used for scheduling to find the near to optimum solution in short time. In a genetic algorithm representation is done with variable length of sub-chromosome. GA is developed to generate

the optimal order scheduling solution. GA is used as tool in different processes to optimize the process parameters. This paper reviews the genetic algorithms that are designed for solving multiple problems in applications of material science and manufacturing in field of mechanical engineering. Genetic algorithm is a multi-path algorithm that searches many peaks in parallel, hence reducing the possibility of local minimum trapping and solve the multi-objective optimization problems. Bejan and Sciubba [31] applied the asymptotic method to determine the optimum geometry of a stack of parallel plates cooled by forced fluid flow. They demonstrated that the thermal conditions of channel walls, with the temperature or flux being constant, don't make much of a difference in the final results. They used a single-objective optimization, and their goal was to increase the amount of heat transfer in the stack of plates. By applying the genetic algorithms, Wei and Joshi [32] minimized the thermal resistance of a micro-channel heat sink. The design variables in their research consisted of some geometrical parameters including the blade thickness, ratio of channel width to blade thickness, etc. They performed their single-objective optimization process by considering two constraints: maximum permitted pressure loss, and maximum permitted inlet flow rate. By combining numerical, analytical and experimental studies and employing the asymptotic analysis method.

To achieve the optimal thermal behaviors in the channels, a multi-objective optimization (MOO) approach should be used to discover the best possible design points with maximum heat transfer and minimum pumping power. NSGAI algorithm (non-dominated sorting genetic algorithm-II) is one of the best and most complete multi-objective optimization algorithms, which will be used in this paper as well. This algorithm was first proposed by Deb et al. [33], and it has been used in recent years in various engineering-related applications, and NSGAI is to find a diverse set of solutions and in converging near the reality optimal set.

3. Results & Discussion

For doing optimization this geometry we should to find optimum mesh element, we checked Nu for mesh element for 7000 to 36000 element. A grid independence procedure is implemented by using the Richards on extrapolation technique over grids with different cell numbers. It is found that the further increase of grid beyond 23,000 cells results in variation in Nusselt number

of less than 1%, thus this grid number is taken as criterion for grid independence (Fig. 3). This fine mesh size will be able to provide good spatial resolution for the distribution of most variables within the channel. The grids were concentrated at the roughened wall region to resolve the high velocity gradient near the wall.

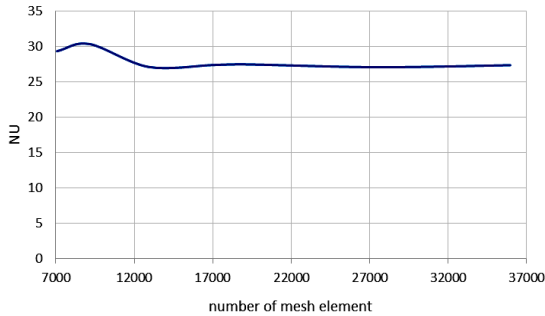


Figure 3: Validation of mesh element for geometry

To be sure of the validity of the numerical modeling used in the optimization process, the obtained numerical results should be compared with similar and available data. In Fig. 4, the variation of Nu number vs Reynolds number has computed for boot shaped ribs and compared with the research of Moon Ma et al [34]. As is observed in Fig 4, present study are accurately match with those of Moon Ma et al [34] and therefore, the present simulation is valid.

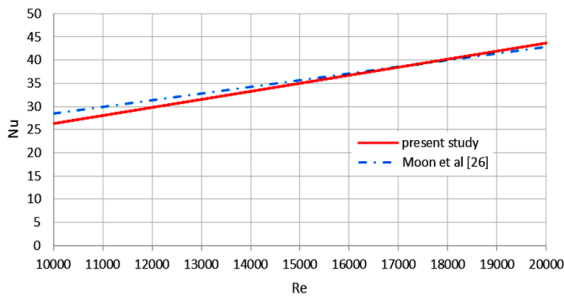


Figure 4: comparison of Nu-Re variation of present study with moon et.al [26]

In order to investigate the optimal distance of between rib groove for different Reynolds, the numerical simulation data are now employed in a multi-objective optimization procedure using NSGA II algorithms. In all runs a population size of 60 has been chosen with crossover probability (Pc) and mutation probability (Pm) as 0.7 and 0.07 respectively. The two conflicting objectives are NU (Nusselt number) and f (friction factor) that should be optimized simultaneously with respect to the design variables d (distance between rib and groove). In this paper Reynolds range of optimization is $5000 \leq Re \leq 30000$ and

optimized point obtained from Genetic algorithm optimization was $2.2w$.

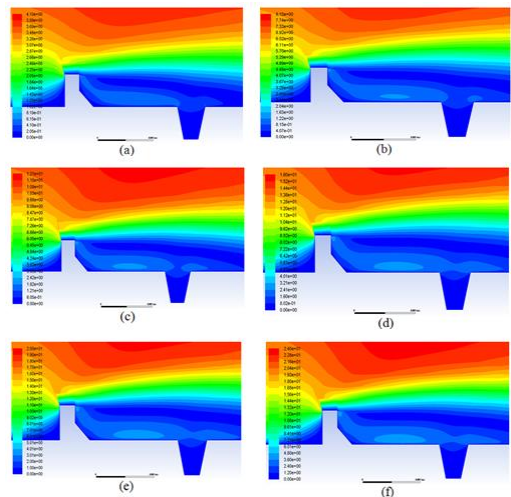


Figure 5: contour of velocity for different Reynolds for optimized point $d=2.2w$ or $7.6(mm)$ (a): $Re=5000$ (b): $Re=10000$ (c): $Re=15000$ (d): 20000 (e): 25000 (f): $Re=30000$

Fig 5 shows contour of velocity for different Reynolds for optimized point, velocity near the walls is zero because condition of fluid flow is no slip and velocity on half of height is maximum when Reynolds number increase flows velocity increase and maximum velocity of fluid flow increase after strike flow with boots rib fluid of flow perverted to up and create vortex after the ribs and in center of vortex velocity is nearly zero

In Table 1 all parameters vs Reynolds number has been shown.

Table 1: Result of optimization for different Reynolds number and $D_{opt}=2.2w$

Re	5000	1000	1500	2000	2500	3000
h ($W m^{-2} K^{-1}$)	13.61	22.62	30.90	38.68	46.77	54.59
Nu	12.81	21.29	29.08	36.40	44.01	53.37
$\Delta P(Pa)$	0.89	5.1	10.4	19.8	32.3	48.4
friction factor	0.24	0.26	0.29	0.31	0.33	0.36

Figure 6 shows streamline of flows near the rib groove for $5000 \leq Re \leq 30000$ when velocity of flows increase vortex length come increase and flow will be more turbulence and destroy laminar sub layer, increasing vortex cause decreasing heat transfer coefficient but if creating vortex cause be more turbulence flow heat transfer

coefficient increases and it's important parameter for increasing heat transfer from hot rib-grooved surfaces.

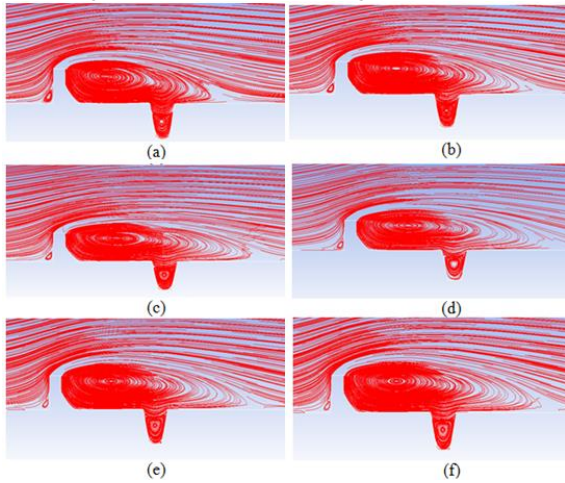


Figure 6: streamline of air for different Reynolds for optimized point $d=2.2w$ or $7.6(\text{mm})$ (a): $\text{Re}=5000$ (b): $\text{Re}=10000$ (c): $\text{Re}=15000$ (d): 20000 (e): 25000 (f): $\text{Re}=30000$

Figure 7 shows temperatures contour of flow near the hot rib grooved surface for different Reynolds number. When velocity of flows increase temperature of heater's wall decrease and temperature of flows increase and heat transfer coefficient and Nusselt number increase.

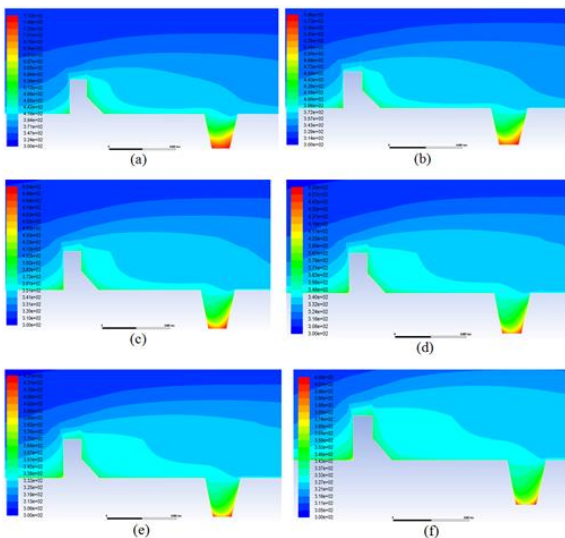


Figure 7: contour of temperature for different Reynolds for optimized point $d=2.2w$ or $7.6(\text{mm})$ (a): $\text{Re}=5000$ (b): $\text{Re}=10000$ (c): $\text{Re}=15000$ (d): 20000 (e): 25000 (f): $\text{Re}=30000$

Figure 8 shows Nusselt number vs distance between rib-grooved for different Reynolds, in $\text{Re}=5000$ Nu is minimum and for $\text{Re}=30000$ Nu is maximum when velocity of flow increase fluid of flow will more turbulence and heat transfer coefficient and the end

Nusselt number increase when distance between rib-grooved increase, Nusselt number increase until $2.2w$ in optimization with NSGAI algorithm point= $2.2w$ is the most optimized other than points for all Reynolds which $5000 \leq \text{Re} \leq 30000$.

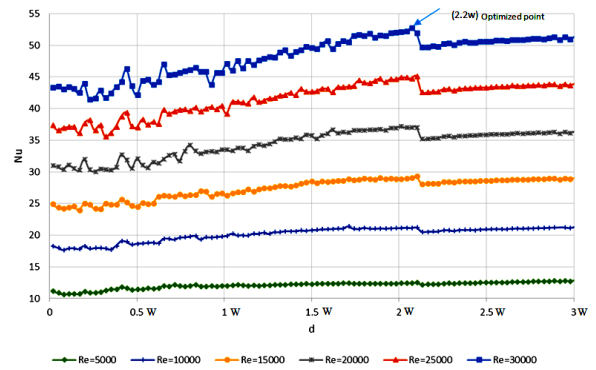


Figure 8: Nusselt vs distance between rib and groove for different Re

Figure 9 shows friction factor vs distance between rib-grooved for different Reynolds, in $\text{Re}=5000$ friction factor is minimum and for $\text{Re}=30000$ friction factor is maximum when velocity of flow increase pressure drop and friction factor increase when distance between rib groove increase friction factor decrease in optimization with NSGAI algorithm point= $2.2w$ is the most optimized than other points for all Reynolds which $5000 \leq \text{Re} \leq 30000$.

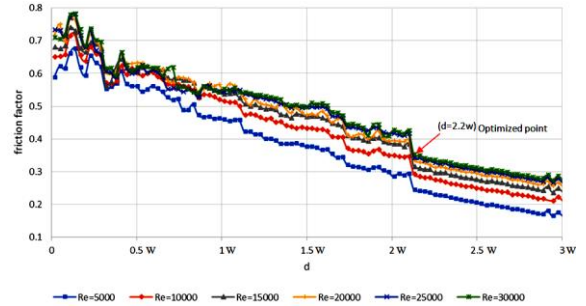


Figure 9: friction factor vs distance between rib and groove for different Re

4. Conclusions

Rib-grooved surfaces are one of the popular techniques that are extensively used in plate heat exchanger manufacturing. In this paper, by combining the CFD approach and the NSGA II algorithm the distance between rib groove ($d=2.2w$) was multi-objectively optimized with considering maximum Nu and minimum friction factor. The governing equations were solved using finite volume

method. Rib grooved channel is a good alternative for high heat flux applications or for more efficient heat exchange devices used in a wide variety of engineering applications like heating and air conditioning units. Also increasing Reynolds number leads to a more complex fluid flow and heat transfer rate.

References

1. Y.M. Zhang, W.Z. Gu, J.C. Han, *Heat transfer and friction in rectangular channels with ribbed or ribbed-grooved walls*, ASME J. Heat Transfer, 1994, 116 - 58–65.
2. Eiamsa-ard, S. and Promvonge, P., *Thermal Characteristic of Turbulent Rib-Grooved Channel Flows*, International Communications in Heat and Mass Transfer, 2009, vol.36, pp. 705-711.
3. Eiamsa-ard, S. and Promvonge, P., *Numerical Study on Heat Transfer of Turbulent Channel Flow Over Periodic Grooves*, International Communications in Heat and Mass Transfer, 2008, vol. 35, pp. 844-852.
4. Kumar, S. and Saini, R. P., CFD Based Performance Analysis of a Solar Air Heater Duct Provided with Artificial Roughness, Renewable Energy, 2009, vol. 34, pp.1285–1291.
5. Varun, Saini, R.P., Singal, S.K., A review on roughness geometry used in solar air heaters. Sol. Energy, 2007, 81, 1340–1350.
6. Patil, A.K., Saini, J.S., Kumar, K., A comprehensive review on roughness geometries and investigation techniques used in artificially solar air heaters. Int. J. Renew. Energy, 2012, Res. 2, 1–15.
7. Prasad, B.N., Thermal performance of artificially roughened solar air heaters. Sol. Energy, 2013, 91, 59–67.
8. Zhongyang Shen a, Yonghui Xie a, Di Zhang b, Numerical predictions on fluid flow and heat transfer in U-shaped channel with the combination of ribs, dimples and protrusions under rotational effects, International Journal of Heat and Mass Transfer, 2015, (80) 494–512.
9. H.T. Wang, W.B. Lee, J. Chan, Numerical and experimental analysis of heat transfer in turbulent flow channels with two-dimensional ribs, Applied Thermal Engineering, 2015, (75) 623e634
10. Saurabh, S., Sahu, M.M., Heat transfer and thermal efficiency of solar air heater having artificial roughness: a review. Int. J. Renew. Energy Res. 2013, 3 (3), 498–508.
11. A.E. Bergles, Recent developments in convective heat transfer augmentation, Applied Mechanics Reviews, 1973, (26) 675–682.
12. R.L. Webb, Principles of Enhanced Heat Transfer, John Wiley Sons, 1994, Chichester,.
13. F.P. Incropera, Convection heat transfer in electronic equipment cooling, Journal of Heat Transfer, 1988, 110 1097–1111.
14. J.C. Han, J.S. Park, Developing heat transfer in rectangular channel with rib tabulator's, Int. J. Heat Mass Transfer, 1988, 31 183–195.
15. S. Fann, W.J. Yang, N. Zhang, Local heat transfer in a rotating serpentine passage with rib-roughened surfaces, Int. J. Heat Mass Transfer, 1993, 37 217–228.
16. T. Liou, J. Hwang, Effect of ridge shapes on turbulent heat transfer and friction in a rectangular channel, Int. J. Heat Mass Transfer, 1993 36 931–940.
17. S.S. Hsieh, H.J. Chin, Turbulent flow in a rotating pass ribbed rectangular channel, ASME J. Heat Transfer, 2003, 125 609–622.
18. Y.H. Liu, M. Huh, J.C. Han, H.K. Moon, High rotation number effect on heat transfer in a triangular channel with 45-deg, inverted 45-deg, and 90-deg ribs, ASME J. Heat Transfer, 2010, 132 paper no. 071702.
19. N.Y. Alkhamis, A.P. Rallabandi, J.C. Han, Heat transfer and pressure drop correlations for square channels with v-shaped ribs at high Reynolds numbers, ASME J. Heat Transfer, 2011, 133 paper no. 111901.
20. J. Lei, J.C. Han, M. Huh, Effect of rib spacing on heat transfer in a two pass rectangular channel (AR = 2:1) at high rotation numbers, ASME J. Heat Transfer 2012, 134 .paper no. 091901.
21. M. Tyagi, S. Acharya, Large eddy simulations of flow and heat transfer in rotating ribbed duct flows, ASME J. Heat Transfer, 2005, (127) 486–498.

22. A.K. Saha, S. Acharya, Turbulent heat transfer in ribbed coolant passages of different aspect ratios: parametric effects, *ASME J. Heat Transfer*, 2007, (129) 449–463.
23. K.R. Aharwal, C.B. Pawar, AlokChaube, Heat transfer and fluid flow of artificially roughened ducts having rib and groove roughness, *Heat Mass Transfer*, 2014, (50)835-847.
24. Anil Kumar , R.P. Saini , J.S. Saini, Heat and fluid flow characteristics of roughened solar air heater ducts-A review. *Renewable Energy*, 2012, (47) 77-94.
25. O.Manca, S.Nardini, D.Ricci, .Numerical study of air forced convection in a rectangular channel provided with Ribs, *Front. Heat Mass Transfer*, 2011.
26. M. A. Moon, M. J. Park, K. Y. Kim, Evaluation of heat transfer performances of various rib shapes, *International Journal of Heat and Mass Transfer*, 2014, 71 275–284.
27. A.R.Jaurker,J.S.Saini,B.K.Gandhi, Heat transfer and friction characteristics of rectangular solar air heater duct using Rib-Grooved artificial roughness, *Sol. Energy*, 2006 , (80)895–907.
28. A. NajahAl-Shamani, K.Sopian, H.A. Mohammed, SohifMat, Mohd HafidzRuslan, Azher M.Abed, Enhancement heat transfer characteristics in the channel with Trapezoidal rib–groove using nanofluids. *Case Studies in Thermal Engineering*, 2015, (5)48–58.
29. B. Bonhoff, S. Parneix, J. Leusch, B.V. Johnson, J. Schabacker, A. Bolcs, Experimental and numerical study of developed flow and heat transfer in coolant channels with 45_ ribs, *Int. J. Heat Fluid Flow*, 1999, 20 (3) 311–319.
30. A. Chaube, P.K. Sahoo, S.C. Solanki, Analysis of heat transfer augmentation and flow characteristics due to rib roughness over absorber plate of a solar air heater, *Renewable Energy*, 2006, (31) 317–331.
31. A. Bejan, E. Sciubba, The optimal spacing of parallel plates cooled by forced convection, *Int. J. Heat Mass Transfer*, 1992, 35 3259-3264.
32. X. Wei, Y. Joshi, Optimization study of stacked micro-channel heat sinks for micro-electronic cooling, *IEEE Transactions Components Packaging Technologies*, 2003, 26- 1.
33. K. Deb, S. Agrawal, A. Pratap, T. Meyarivan, A fast and elitist multi-objective genetic algorithm: NSGA-II”, *IEEE Trans Evolutionary Computation*, 2002, (6) 182-197.
34. Mi-Ae Moon, Min-Jung Park, Kwang-Yong Kim, Evaluation of heat transfer performances of various rib shapes, *International Journal of Heat and Mass Transfer*, 2014, 275-284.